33rd European Modeling & Simulation Symposium
18th International Multidisciplinary Modeling & Simulation Multiconference

ISSN 2724-0029 ISBN 978-88-85741-57-7 © 2021 The Authors.
doi: 10.46354/i3m.2021.emss.046

Integrated optical gas sensor based on O-ring resonator and loop waveguide mirror on silicon nitride platform

Anna Elmanova[1*], Ilia Elmanov[1], Vadim Kovalyuk[1], Pavel An[1] Galina Chulkova[1,2] and Gregory Goltsman[1,2]

[1]Department of Physics, Moscow Pedagogical State University (MPGU), 119992, Russia
[2]National Research University Higher School of Economics, Moscow 101000, Russia
*Email address: anna.elmanova.belskaya@gmail.com

Abstract

A model of an integrated photonic device based on an O-ring resonator and loop waveguide reflector operated at telecom wavelength (1550 nm) was developed. A well-studied model of the O-ring resonator was used, and added a waveguide loop mirror to reflect radiation to input. The loop design was altered by varying the distance between the loop and the ring resonator. The obtained results can be used for gas-sensing aims if a device is coupled only with one optical fiber, both an input and an output. Such a device can be used in hard-to-reach places where the presence of a person is not desirable or may be even dangerous.

Keywords: Photonic integrated circuit; Oring resonator; Loop waveguide reflector; Gas-sensing

1. Introduction

Photonic integrated circuits are currently under active research (Dong et al., 2010). The application of such circuits in gas-sensing is of special interest (Green et al., 2019). Several studies have been carried out on how various nanophotonic devices can be used to determine the change in the refractive index of the environment (Sharma et al., 2020). Different platforms are studied for these purposes, such as silicon on insulator, lithium niobate on insulator, A_3B_5, Al_2O_3, different polymeric materials (Staline & Shanmuganantham, 2014, Udrea & Gardner, 2002, Li et al., 2016, Clevenson et al., 2013). Due to the wide spectral range of operation, including the visible and infrared range, and the CMOS compatible fabrication process, silicon nitride as a waveguide material is very prospective (Muñoz et al., 2017). Numerous photonic integrated devices have already been developed for this platform, such as O-ring resonators with different parameters (Koushik & Malathi, 2019), Bragg waveguides, spiral resonators (Kohler et al., 2020), Mach-Zehnder interferometers (Antonacci et al., 2020).

The present work was held based on already carried out experiments with silicon nitride O-ring resonator for gas-sensing applications (Elmanova et al., 2020), where sensitivity has been demonstrated to gases having both higher and lower refractive indices than air. But to make a finished device, it must be strictly coupled with optical fiber. Working with nanophotonics integrated circuits needs the precise imposition of the optical fiber array with integrated photonic devices (Bernabé et al., 2012). To solve the problem, usually, the expensive piezo-motors are used (Brahim, 2017). Another possible solution to the

problem is to use a micromechanical system to impose a separate optical fiber with a single photonic device (Bogucki et al., 2018, Wan et al., 2019). Whichever method of alignment is used, the possibility of using only one optical fiber would lead to a reduction in the cost and simplification of the gas sensing circuit using the most sensitive element of an O-ring resonator with a high Q-factor. In this case, developing such a device will present not the transmission spectra but the reflection. A spattered golden mirror can be used (Manolis et al., 2019). These mirrors were presented to be used as parts of interferometers without implementation to any sensing device. But if a decision is made to use golden mirrors in optical circuits, this adds another step to the technological route, complicating the fabrication of such a photonic circuit. However, the presence of a loop waveguide mirror increases the sensitivity of the device, which also corresponds to gas-sensing aims (Kou, Xu & Lu, 2012).

We decided to study a device consisting of a waveguide reflector and an O-ring resonator as a gas-sensor. The dependences of the main parameters of a sensor, such as full width at half maximum (FWHM) and free spectral range (FSR) from the design of the waveguide loop and its position relative to the O-ring resonator were studied. The designed devices were investigated for different refractive indices of the surroundings. As a result, the design for such a device that can be used for gas-sensing applications with a combined optical input and output was obtained.

2. State-of-the-art

The use of ring resonators as gas sensors is ubiquitous and has been developing especially actively recently. Ring resonator gas sensor has been introduced as widely applicable devices. They are common for both organic and inorganic compound detection (Luan et al., 2018). Refractive index sensing is important nowadays and a common way to develop different integrated photonic chemical sensors (Passaro et al., 2012). It occurs throughout evanescent electric field mode, as the waveguide mode is not sensible to the changes in the refractive indices of the surroundings. Therefore, studying ring resonators as refractive index sensors is an important problem in integrated photonics. The sensitivity of the ring resonator devices can be up to 200 ppm (Sun & Fan, 2008). The most important features of the ring resonators are their high performance, easy fabrication with a low percentage of inaccuracies, and the possibility to highly vary their properties by changing radii and gap (Lydiate, 2017). As far as the devices are common, their simulation is also a subject of fluent studies (Barrios, 2009). There are different ways to simulate transmission in a ring resonator and its applicability for gas-sensing aims. The first approach to determining the ring resonator parameters usesgeneral equations for the electric field propagation (de Leonardis et al., 2017). The formula can simplify the picture and introduce the radius, the gap, and the width of the resonator for a peculiar case. Then the parameters of the devices can be introduced more accurately throughout performing mathematical simulations. There are two main approaches to the problem, and some authors prefer FEM computations (Haas et al., 2019) while others prefer FDTD (Niegemann et al., 2009). In general, both approaches are adequate, even though FDTD is more applicable for complicated circuits.

Loop waveguide mirrors are prospective devices for photonic applications. They are not very common. Usually, there are golden mirrors in different interferometer circuits (Sulaiman et al., 2020). An interesting application of the device is opened whenever one considers its resonant properties(Mitarai et al., 2019). Optical loop mirrors may be processed on a silicon nitride platform (Wang et al., 2018and can be integrated with other elements of photonic circuits. The loop waveguide mirror is an important device whenever one needs to obtain the transmission and the reflection picture. This can happen in the case of combined input and output of the circuit. An interesting attempt to integrate the loop mirror with a ring resonator was performed on the silicon-on-insulator platform (Mitarai et al., 2020). The authors claim that the devices make a better resolution than the ordinary ring resonator. The device was developed for work on the 1550 nm wavelength. But the authors use separated input and output and the loop mirror only as a kind of a filter.

One of the important properties of a loop waveguide mirror is its ability, as for almost any resonant cavity, to sense changes in the refractive index of the surroundings throughout the evanescent field mode (Kou et al., 2012). The sensitivity of a slot loop waveguide introduced in the paper is up to 6×10^3 nm per refractive index unit (RIU), making the device significantly applicable for chemical sensing aims. The finite element method (FEM) for numerical simulations was taken to verify the loop mirror sensing properties. Here, the reflection of the device on one single wavelength is mostly studied, which is much more convenient to be held via the FEM method.

The novelty of the presented paper lies in the fact that there were no circuits introduced with coupled ring resonators and waveguide loop mirrors on silicon nitride platform for operation in the telecom wavelength range with combined input and output port. The studied device may introduce novel paths in refractive index sensing. Both devices included in the circuit are simple in fabrication, and their properties can be easily varied throughout their geometrical parameters.

3. Materials and Methods

A device with a golden mirror at the end of the rectilinear waveguide was examined, and its behavior was compared with the waveguide ending with a loop reflector. The reflectance spectra for both were used,

and they were found out to be similar. In the numerically studied model, the parameters of the commercially available silicon nitride wafers with thermal silicon oxide SiO_2=2.6 μm and half-etched silicon nitride Si_3N_4=450 nm layers atop were used. The final device consisted of a rectilinear waveguide with a loop waveguide mirror at the end.

The reflection port was studied for the carried simulations. TheFEM in COMSOL Multiphysics and finite difference time domain method (FDTD) (Taflove & Hagness, 2005), implemented in an open-source package MEEP (Oskooi et al., 2010) were used to develop the O-ring resonator and the loop waveguide mirror first separately, then as a combined photonic circuit. The applications of the methods deeply varied depending on the devices simulated. In general, the FDTD method is more convenient for complicated photonic circuits simulations, especially when considering a wide wavelength range. On the other hand, computation of the reflectance for a simple device on one wavelength is much easy using the FEM method. Therefore, the perfect golden mirror and the loop waveguide reflectance (Figure 1a), the electric field propagation picture (Figure 1b, c), and the single-mode electric field distribution were calculated based on FEM. All the waveguides were set to 1 μm width for the linear parts and 1.6 μm for the ring. This width for the ring resonator, together with its radius being 63.728 μm and the gap between the rectilinear waveguide and the ring equal to 1.4 μm, were already described in Elmanova et al., 2020 and proven experimentally to give sensitivity up to 2.23 × 105 ppm for Helium. The reflected light intensity of the loop waveguide is comparable, and the overall losses are negligible compared to the golden ring with linear sizes of 20 μm. The finished device with the loop waveguide mirror, and ring resonator was simulated using the FDTD method.

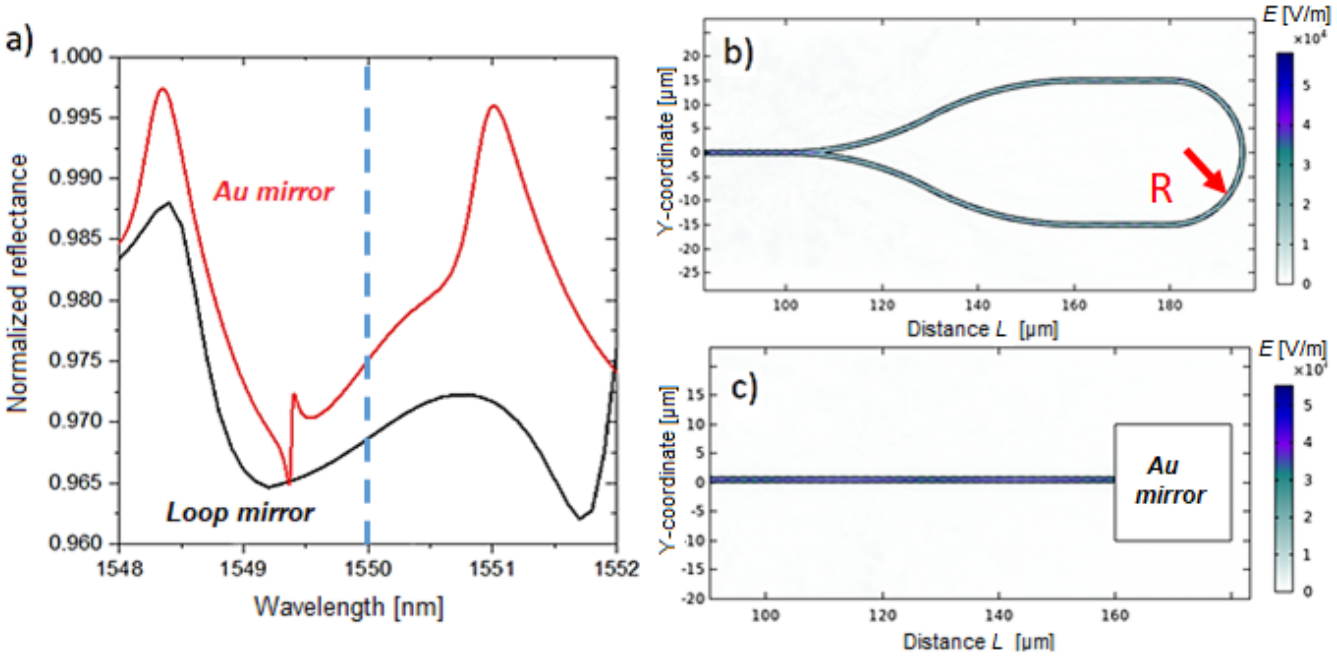

Figure 1. a) Comparison of reflective characteristics, obtained using COMSOL, for a golden mirror and a loop waveguide of radius 30 μm and length 60 μm. Both plots are close to the unit, which shows good properties for a reflector. b) Electric field propagation in the waveguide Loop mirror simulated by FEM. c) Electric field propagation up to the square golden mirror simulated by FEM.

4. Simulation

In the first step, the radiation propagation through the rectilinear waveguide with a loop waveguide mirror was studied and, separately, through a waveguide with a golden reflector

(Figure 1c) using the FEM method in COMSOL Multiphysics. Corresponding two-dimensional models of the simplest square gold mirror with a linear size of 20 μm and a loop waveguide were developed. This device is a straight-line waveguide ending with a Y-splitter with a division ratio of 50/50. After the splitter, there is a rectilinear waveguide section of length *L*. The two waveguides are closed by a ring of radius *R*. Thus, two main parameters of the loop waveguide are introduced. The results obtained indicate that the radiation almost totally reflects in both cases (in the range of 96-99.6%). Also, the design of the loop was varied so that the reflection spectrum was lesser deviated from unity. To perform simulations in COMSOL and MEEP, the effective refractive indices method was used to perform two-dimensional computations (Chiang, 1991). As the Radius of the Loop and its length were altered in a range from 5 to 35 μm,

and the reflectance on the wavelength 1550 nm was obtained (Figure 2a). The loop with a high radius, more than 30 μm (Figure 2b), shows a poor performance due to the long pathway and, therefore, losses increase. A too-small radius (Figure 2c), on the other hand, does not allow enough radiation to come back to the linear waveguide, and the performance is high only in a narrow range of the loop lengths. The condition for high reflectance was found to be the radius of the loop between 15 and 25 μm while the loop length should be between 10 and 30 μm.

In the second step, the parameters for the O-ring resonator were determined, and the two elements were combined. For the device, the simulations were held for two different refractive indices with a difference of 0.001 to determine the possible application as a refractive index sensor. The obtained reflectance plots present that the device is sensitive to the changes in the refractive index. Therefore, it can be used as a gas sensor. The curve obtained had a noticeable difference in the behavior of different resonant peaks. Therefore, these plots were compared with the reflectance of the loop separated and the transmission of the ring separated. Furthermore, their behavior was studied independently. Such parameters as the full width at half maximum (FWHM), free spectral range (FSR), finesse, and quality factor (Q-factor) were taken for the loop curve and the ring curve. These values were compared, and their dependences on the distance between the beginning of the loop (the starting point of the Y-splitter) and the central ring resonator point were plotted (Figure 3d). The losses are low enough for the device to be applied for sensing aims.

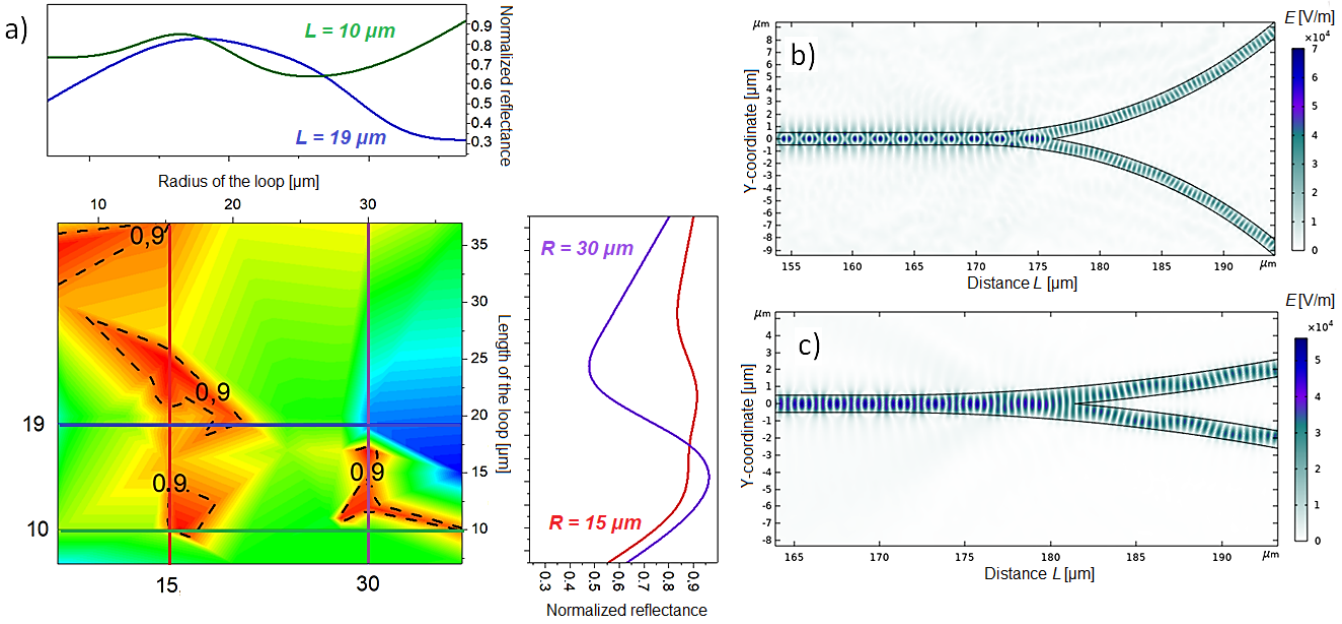

Figure 2. a) Color contour map for the relative reflection of the Loop dependence on the radius of the loop and its length for an array of 8×8 points. The profile curves are also depicted for some specific values. The reflection higher than 0.9 is separated with a dashed line. b) Transition of an electric field from a linear waveguide to a loop throughout a Y-coupler when the radius of the loop is higher than 15 μm simulated with COMSOL Multiphysics. c) Transition of an electric field from a linear waveguide to a loop throughout a Y-coupler when the radius of the loop is less than 5 μm simulated with COMSOL Multiphysics.

5. Results and Discussion

Using the numerical FEM and FDTD methods, the dependences of the reflectance from the device on different parameters were simulated. The radius of curvature and the length of the loop were varied to get a better reflection. The best performance was shown for the loop with a curvature radius of 30 μm, length of the loop 85 μm. For the O-ring resonator (apart from the whole device), the gap between the ring and the bus waveguide was varied, considering the radius of 100 μm. The obtained gap for the best performance was found to be 0.3 μm (Figure 3b). The distance between the loop and the ring was swept for the whole device, and the optimal distance through the Lorentz fit of the reflectance curves was found to be more than 60 μm (Figure 3d). The waveguide width for the resonator was 1.8 μm, and for the waveguide structures, 1 μm. Some of the obtained resonance peaks appeared due to the operation of the ring resonator, and some were due to the addition to the system of the loop waveguide (Figure 3c). The dependence of the parameters of the device on the distance between the loop and the ring *L* (which was varied from 40 to 90 μm) showed a stable picture when the distance is higher than 50-60 μm. This also coincides with theory, as the ring resonator has a lower influence on the loop and vice versa. The Q-factor and finesse (Fig. 3d) for the system without loop mirror and its addition are stable and high enough for

studies. Even though a low contrast in refractive indices, the device has proven itself to have low optical losses. The loop reflectance was shown higher than 0.9 from the input radiation, and for the resultant device, the reflection was shown to be up to 0.8, which is also a reasonable result. The resonant peaks for the ring resonator had lower FWHM but higher finesse, Q-factor, FSR, and sensitivity than the loop resonances, which only outrange rings in the FWHM. Still, it is important to use both devices. A full on-chip sensing laboratory can be developed using ring resonators and loop waveguides of different parameters. A ring resonator and a loop waveguide mirror system showed the appearance of the new resonant peaks, which are more sensitive to changes in the refractive index. The device has shown 140 nm/RIU sensitivity for the system of the ring resonator with the loop mirror. The separated ring resonator has the sensitivity of only 20 nm/RIU due to the resonant peak shift. Therefore, the system of a ring resonator with a loop waveguide mirror is seven times more sensible.

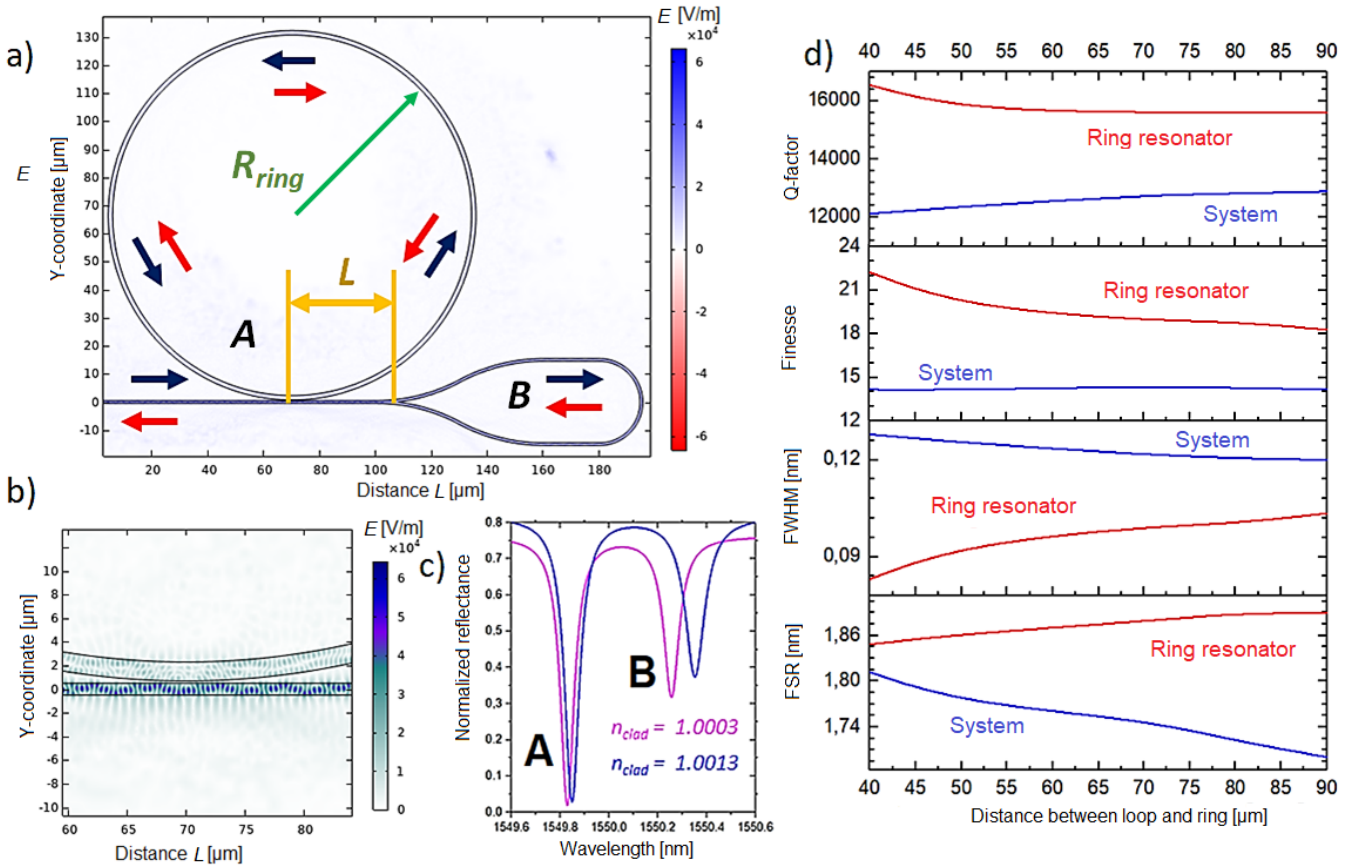

Figure 3. a) General view of electric field (z-component) propagation in the device simulated using FEM. The blue arrows indicate the forward path of optical radiation; the red ones show the backward path. The distance between loop and ring is denoted. b) Transition of an electric field from a linear waveguide to a ring resonator by FEM. c) The normalized reflectance spectra obtained in MEEP for the device at different refractive indices of the surroundings when the distance between the loop and the mirror equals 70 μm. With capital «A» the resonant peak from the O-Ring resonator is denoted, and the peak that appears when the loop is added to the ring resonator as «B». d) Different properties of the reflection resonant curves for the ring resonator and for the system with both ring and loop depending on the linear distance between the loop and the ring.

The parameters were derived so that at a wavelength of about 1550 nm (exactly 1549.8 nm and 1550.3 nm), there were two of the resonance peaks, and the Lorentz fit gives the values of FWHM = 0.734 nm, FSR = 1.873 nm for n = 1.0003 and FSR = 1.85 nm for n = 1.0013.

6. Conclusions

A gas sensor based on a silicon nitride platform, consisting of a waveguide loop mirror and an O-ring resonator, was studied in this work. The work was performed using FEM and FDTD numerical methods. By varying parameters such as the gap between the waveguide and the ring, the distance between the loop and the ring, and the radius of the loop, the optimal configuration of these parameters was found. Further work will be devoted to the fabrication of the device and its experimental study. The device is designed to be fabricated and easily integrated with other different photonic integrated circuits. It is important to develop different integrated photonic circuits on silicon nitride platforms as gas sensors as they are easily fabricated and very sensitive to changes in the refractive indices of the surroundings. The ring resonator integrated with

the loop mirror showed high performance and needed experimental verification.

Funding

The research was performed in support of the Russian Science Foundation grant No. 19-72-10156.

References

Antonacci, G., Goyvaerts, J., Zhao, H., Baumgartner, B., Lendl, B. & Baets R. (2020) Ultra-sensitive refractive index gas sensor with functionalized silicon nitride photonic circuits. *APL Photonics, 5, 081301.*

Barrios, C. A. (2009). Analysis and modeling of a silicon nitride slot-waveguide microring resonator biochemical sensor. *Optical Sensors 2009. Published.*

Bernabé, S., Kopp, K., Volpert, M., Harduin, J., Fédéli, J. M. & Ribot, H. (2012) Chip-to-chip optical interconnections between stacked self-aligned SOI photonic chips. Opt. Express 20, 7886-7894.

Bogucki, A., Zinkiewicz, L., Pacuski, W., Wasylczyk, P. & Kossacki, P. (2018) Optical fiber micro-connector with nanometer positioning precision for rapid prototyping of photonic devices. *Opt. Express, 26, 11513-11518.*

Brahim M. (2017) Modeling and Position Control of Piezoelectric Motors. *Université Paris Saclay (COmUE).*

Chiang, K. S. (1991) Effective-index method for the analysis of optical waveguide couplers and arrays: an asymptotic theory. *Journal of Lightwave Technology, 9, 1, 62-72.*

Clevenson, H., Desjardins, P., Gan, X. & Englund, D. (2013) Gas sensing using a resilient polymer photonic crystal nanocavity with ultra-high quality factor. *CLEO, OSA Technical Digest, AF1J.2.*

De Leonardis, F., Soref, R. A., & Passaro, V. M. N. (2017). Investigation of Electric Field Induced Mixing in Silicon Micro Ring Resonators. *Scientific Reports, 7(1).*

Dong, P., Chen, Y. K., Duan, G. H. & Neilson, D. (2014). Silicon photonic devices and integrated circuits. Nanophotonics. *3, 10.1515/nanoph-2013-0023.*

Elmanova, A., An, P., Kovalyuk, V., Golikov, A., Elmanov, I., Goltsman, G. (2020) *J. Phys.: Conf. Ser., 1695, 012124.*

Green, W., Zhang, E., Xiong, C., Y. Martin, J. Orcutt, M. Glodde, L. Schares, T. Barwicz, C. Teng, N. Marchack, E. Duch, S. Kamlapurkar, S. Engelmann, N. Hinds, T. Picunko, R. Wilson, and G. Wysocki. (2019) Silicon Photonic Gas Sensing. *Optical Fiber Communication Conference (OFC), OSA Technical Digest (Optical Society of America, 2019), paper M2J.5.*

Haas, J., Artmann, P., & Mizaikoff, B. (2019). Mid-infrared GaAs/AlGaAs micro-ring resonators characterized via thermal tuning. *RSC Advances, 9(15), 8594–8599.*

Kohler, D., Allegro, I., Wondimu, S. F., Hahn, L., Freude, W., and Koos, C. (2020) Lasing in Si3N4-organic hybrid (SiNOH) waveguides. *Opt. Express, 28, 5085-5104.*

Kou, J, Xu, F & Lu, Y. (2012) Loop-mirror-based slot waveguide refractive index sensor. *AIP, Adv., 2, 042142.*

Koushik, K. P. & Malathi, S. (2019) Dual Ring Resonator for Gas Sensing Application. *WRAP, 2019, 1-2.*

Li, X., Mu, Z., Hu, J. & Cui, Z. (2016) Gas sensing characteristics of composite NiO/Al2O3 for 2-chloroethanol at low temperature. *Sensors and Actuators B: Chemical, 232, 143-149.*

Luan, E., Shoman, H., Ratner, D., Cheung, K., & Chrostowski, L. (2018). Silicon Photonic Biosensors Using Label-Free Detection. *Sensors, 18(10), 3519.*

Lydiate, J. (2017). Modelling and simulation of a thermally induced optical transparency in a dual micro-ring resonator. *Royal Society Open Science, 4(7), 170381.*

Manolis, A., Chatzianagnostou, E., Dabos, G., Pleros, N., Chmielak, B., Giesecke, A. L., Porschatis, C., Cegielski, P. J., Markey, L., Weeber, J. C., Dereux, A. & Tsiokos, D. (2019) Plasmonic stripes integrated in a silicon nitride Mach Zehnder Interferometer for high sensitivity refractometric sensors. *Conference on Lasers and Electro-Optics, OSA Technical Digest, JTh2A.94.*

Mitarai, T., Eissa, M., Miyazaki, T., Amemiya, T., Nishiyama, N., & Arai, S. (2019). Broadband Si waveguide loop mirror with curved directional coupler. *2019 24th OptoElectronics and Communications Conference (OECC) and 2019 International Conference on Photonics in Switching and Computing (PSC). Published.*

Mitarai, T., Moataz, E., Miyazaki, T., Amemiya, T., & Nishiyama, N. (2020). Design and measurement of broadband loop mirror with curved directional coupler based on Si waveguides. *Japanese Journal of Applied Physics, 59(11), 112002.*

Muñoz, P., Micó, G., Bru, L., Pastor, D., Pérez, D., Doménech, J., ... Domínguez, C. (2017). Silicon Nitride Photonic Integration Platforms for Visible, Near-Infrared and Mid-Infrared Applications. *Sensors, 17(9), 2088.*

Niegemann, J., Pernice, W., & Busch, K. (2009). Simulation of optical resonators using DGTD and FDTD. *Journal of Optics A: Pure and Applied Optics, 11(11), 114015.*

Oskooi, A., Roundy, D., Ibanescu, M., Bermel, P., Joannopoulos, J.D. & Johnson, S.G. (2010) MEEP: A flexible free-software package for electromagnetic simulations by the FDTD method. *Computer Physics*

Communications, 181, 687-702.

Passaro, V., Tullio, C., Troia, B., Notte, M., Giannoccaro, G., & Leonardis, F. (2012). Recent Advances in Integrated Photonic Sensors. *Sensors, 12(11), 15558–15598.*

Sharma, T., Wang, J., Kaushik, B. K., Cheng Z., Wei, Z. & Li, X. (2020) Review of Recent Progress on Silicon Nitride-Based Photonic Integrated Circuits. IEEE Access, 8, 195436-195446.

Staline, J., Shanmuganantham, T. (2014) Design And Analysis Of Saw Based Mems Gas Sensor For The Detection Of Volatile Organic Gases *IJERA, 4, 3, 254-258.*

Sulaiman, A. H., Yusoff, N. M., Abdullah, F., & Mahdi, M. A. (2020). Tunable multiwavelength fiber laser based on bidirectional SOA in conjunction with Sagnac loop mirror interferometer. *Results in Physics, 18.*

Sun, Y., & Fan, X. (2008). Analysis of ring resonators for chemical vapor sensor development. *Optics Express, 16(14), 10254.*

Taflove, A. & Hagness, S.C. (2005) Computational Electrodynamics: The Finite-Difference Time-Domain Method. *Artech: Norwood, MA.*

Udrea, F. & Gardner, J. W. (2002) SOI CMOS gas sensors. *SENSORS, IEEE, 2, 1379-1384.*

Wan, C., Gonzalez, J. L., Fan, T., Adibi, A., Gaylord, T. K. & Bakir, M. S. (2019) Fiber-Interconnect Silicon Chiplet Technology for Self-Aligned Fiber-to-Chip Assembly. *IEEE Photonics Technology Letters, 31, 16, 1311-1314.*

Wang, Z., Glesk, I., & Chen, L. R. (2018). An integrated nonlinear optical loop mirror in silicon photonics for all-optical signal processing. *APL Photonics, 3(2), 026102.*